Journal of Alloys and Compounds 509 (2011) 3985–3990

Contents lists available at ScienceDirect

Journal of Alloys and Compounds

journal homepage: www.elsevier.com/locate/jallcom

Effects of α- and β-Si_3N_4 as precursors on combustion synthesis of (α + β)-SiAlON composites

C.L. Yeh*, F.S. Wu, Y.L. Chen

Department of Aerospace and Systems Engineering, Feng Chia University, 100 Wenhwa Road, Seatwen, Taichung 40724, Taiwan

ARTICLE INFO

Article history:
Received 12 November 2010
Received in revised form
24 December 2010
Accepted 29 December 2010
Available online 4 January 2011

Keywords:
Ceramics
Gas–solid reactions
X-ray diffraction
(α + β)-SiAlON
Combustion synthesis

ABSTRACT

Preparation of (α + β)-SiAlON composites from the powder compacts of Si, Si_3N_4, SiO_2, Al, and AlN was investigated by self-propagating high-temperature synthesis (SHS) in nitrogen of 2.17 MPa. Test samples adopted not only pure α- and β-Si_3N_4, but also a mixture of (α + β)-Si_3N_4. The combustion temperature and flame-front propagation velocity decreased with increasing ratio of Si/Si_3N_4, but they increased with proportion of α/β-Si_3N_4. For the sample containing pure α-Si_3N_4, the synthesis reaction yielded only α-SiAlON with various morphologies including equiaxed crystals, elongated grains, and fine whiskers. As a mixture of (α + β)-Si_3N_4 was employed, the resulting products were (α + β)-SiAlON composites, within which the content of β-SiAlON increased with increasing β-Si_3N_4. For the sample adopting 100% β-Si_3N_4, comparable amounts of α- and β-SiAlON were produced. Additionally, the morphology of (α + β)-SiAlON composites was dominated by elongated grains with a high aspect ratio.

1. Introduction

Sialon has been considered as a promising high-temperature structural material and a superior tribological ceramic, owing to its excellent mechanical properties and chemical stability [1–5]. The high hardness, fracture toughness, and thermal shock resistance make sialon well suited to replace cemented carbides as cutting tools in machining nickel-based superalloys. There are two well-known sialon phases, α- and β-SiAlON, which are solid solutions based upon structural modifications of α- and β-Si_3N_4, respectively. The general formulas of α- and β-SiAlON are expressed correspondingly as $Me_{m/v}Si_{12-(m+n)}Al_{m+n}O_nN_{16-n}$ (Me stands for an interstitial metal ion of valence v) and $Si_{6-z}Al_zO_zN_{8-z}$ ($0 < z \leq 4.2$). The α phase of SiAlON is normally in the form of equiaxed grains and features high hardness, good wear and oxidation resistance, and excellent thermal shock resistance, whereas β-SiAlON appears as elongated grains and is characterized by good fracture toughness [4,5]. Recently, both α- and β-SiAlON have been employed as host lattices for rare-earth cations to generate efficient luminescence [6–9]. The combination of high thermal and chemical stabilities and excellent luminescence properties renders sialon a novel functional application in displays and white light-emitting diodes (LEDs) [6–9].

Fabrication of α- and β-SiAlON has been conducted by a variety of processing routes, such as hot isostatic pressing (HIP) [2,4], hot pressing (HP) [10–12], gas pressure sintering [7–9,13], pressureless sintering [14], liquid-phase sintering [15], carbothermal reduction and nitridation (CRN) [16,17], and combustion synthesis [18–25]. For example, Mandal [4] prepared different α-SiAlONs using Si_3N_4, AlN, Al_2O_3, and Me_xO_y (where Me = Sr, Ca, La, Ce, Nd, and Yb) by HIP at 1800 °C for 2 h, and observed an elongated morphology in the (Nd + Ca)- and (Ce+Ca)-doped products. Shen et al. [11] obtained Yb-stabilized α-SiAlONs with a wide range of compositions by hot pressing the powder mixture of Si_3N_4, AlN, Al_2O_3, SiO_2, and Yb_2O_3 at 1800 °C and 25–32 MPa for 2 h. By using α-Si_3N_4, Al_2O_3, AlN, and Eu_2O_3 powders under nitrogen of 0.5 MPa, Zhu et al. [7] produced Eu^{2+}-doped β-SiAlON phosphors in a sintering furnace at 1900 °C for 3 h. Haviar [13] showed that for the sintering temperature below 1500 °C a decrease in the precursor proportion of α/β-Si_3N_4 enhanced the formation of β-SiAlON that was converted to the α phase at the temperature above 1600 °C. Zhou et al. [14] fabricated α-SiAlON by pressureless sintering of α-Si_3N_4, Al_2O_3, and Y_2O_3 powders at 1050 °C in nitrogen of 0.1 MPa for 2 h and observed elongated α-SiAlON well distributed in a matrix of equiaxed grains. When compared with combustion synthesis, the above-mentioned methods are highly time-consuming and energy-intensive.

Combustion synthesis in the mode of self-propagating high-temperature synthesis (SHS) takes advantage of the self-sustaining merit from highly exothermic reactions, and hence, has the benefits of low energy requirement, short processing time, and sim-

* Corresponding author. Tel.: +886 4 24517250x3963; fax: +886 4 24510862.
E-mail address: clyeh@fcu.edu.tw (C.L. Yeh).

0925-8388/$ – see front matter © 2011 Elsevier B.V. All rights reserved.
doi:10.1016/j.jallcom.2010.12.201

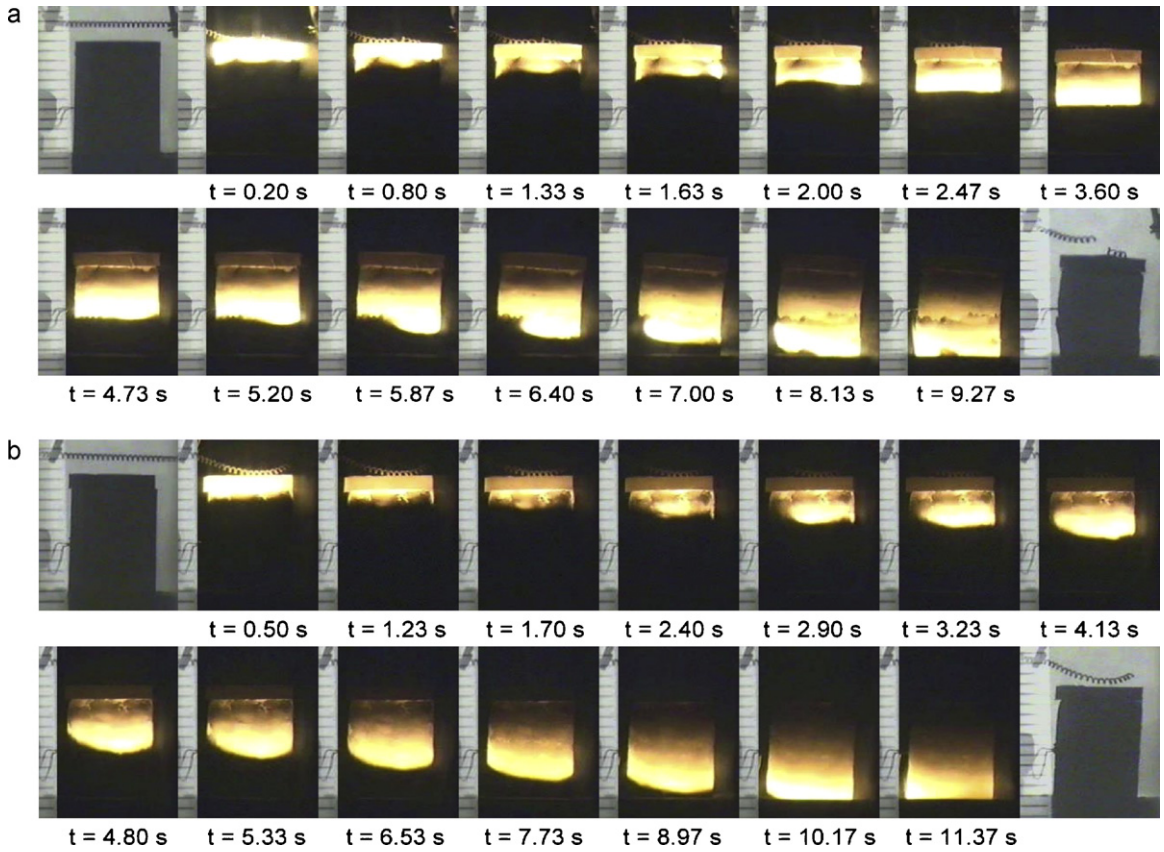

Fig. 1. Sequences of recorded images illustrating self-sustaining combustion along samples of SA1 with different proportions of α-Si_3N_4:β-Si_3N_4 = 80:20 (a) and 20:80 (b).

ple facilities [26–29]. Liu and co-workers [18–21] conducted a series of combustion studies on the preparation of various α-SiAlONs from different Me_xO_y–Si–Si_3N_4–(SiO_2)–Al–(AlN) systems. They indicated that the rapid heating rate and short reaction time of combustion synthesis and the additives like Fe_2O_3 and NH_4F were beneficial for the growth of rod-like α-SiAlON crystals [18–21]. By activating the raw materials including Si, Al, and SiO_2 powders in a planetary ball mill for 1–10 h, Yi and Akiyama [22] fabricated β-SiAlON powders through SHS in nitrogen of 0.7–2.5 MPa. The β phase of SiAlON with z = 3 and 4 was also produced by combustion synthesis using mechanically activated Si, Al, and Al_2O_3 powders in nitrogen of 1 MPa [24]. Recently, Yeh and Sheng [25] produced elongated Yb α-SiAlON by SHS from the powder compacts with α-Si_3N_4/Si = 0.4–0.5 in nitrogen of 2.17 MPa, while the α-SiAlON in the form of equiaxed gains was synthesized from the samples with AlN/Al = 0.85–1.0.

In view of the fact that α- and β-SiAlON are completely compatible to form a composite material with good mechanical properties from their monolithic counterparts, the composite of (α + β)-SiAlON has received increasing attention [4]. The objective of this study aims to investigate the influence of α- and β-Si_3N_4 as the precursors on the phase and morphology of SiAlON produced through combustion synthesis in the SHS mode under gaseous nitrogen. Unlike the previous study preparing α-SiAlON [25], this study is focused on formation of the (α + β)-SiAlON composite. The powder compacts were formulated with different molar ratios of Si/Si_3N_4 and various proportions of α/β-Si_3N_4. In addition, the effect of sample stoichiometry was explored on the combustion characteristics, including the propagation mode of self-sustaining combustion, flame-front propagation velocity, and combustion temperature.

2. Experimental methods of approach

The starting materials of this study included Yb_2O_3 (Strem Chemicals, 99.9%), Si (Strem Chemicals, ≤45 μm, 99%), α-Si_3N_4 (Aldrich, ≤45 μm, 99%), β-Si_3N_4 (Aldrich, ≤45 μm, 99%), SiO_2 (Aldrich, ≤45 μm, 99.6%), Al (Showa Chemical Co., 10 μm, 99.9%), and AlN (Strem Chemicals, 99%). The powder mixture was formulated according to the composition of Yb-stabilized α-SiAlON, $Yb_{m/3}Si_{12-(m+n)}Al_{m+n}O_nN_{16-n}$, with m = 1.6 and n = 1.0. Table 1 lists five different starting stoichiometries of the samples (labeled by SA1–SA5), within which the molar ratio of Si/Si_3N_4 varies from 2.5 to 4.5. It should be noted that Si_3N_4 used in the sample can be the α or β phase, or a mixture of both. When green samples with mixed α- and β-Si_3N_4 powders were prepared, the proportion of α/β-Si_3N_4 ranged between 20/80 and 80/20. The reactant powders were dry mixed in a ball mill and isostatically cold-pressed into cylindrical samples with a diameter of 7 mm, a height of 12 mm, and a compaction density of 40% relative to the theoretical maximum density (TMD).

The SHS experiments were conducted in a stainless-steel windowed combustion chamber under a nitrogen pressure of 2.17 MPa. The nitrogen gas had a purity of 99.999%. The sample holder was equipped with a 600 W cartridge heater for raising the initial temperature of the sample prior to ignition. In this study, a preheating temperature of 150 °C was required to assure self-sustaining combustion of the reactant compact. Moreover, a compacted pellet (2 mm in height and 7 mm in diameter) made up of the powder blend of titanium and carbon (with a molar ratio of Ti:C = 1:1) was placed on the top of the test specimen to serve as an ignition enhancer which was

Table 1
Summary of starting compositions of test samples for combustion synthesis of (α + β)-SiAlON composites.

Samples	Compositions (mol%)					
	Yb_2O_3	Si	Si_3N_4	SiO_2	Al	AlN
SA1	3.00	47.58	19.02	1.13	20.91	8.36
SA2	2.91	50.74	16.90	1.09	20.26	8.10
SA3	2.83	53.26	15.20	1.06	19.76	7.89
SA4	2.77	55.27	13.80	1.04	19.36	7.76
SA5	2.72	57.00	12.65	1.02	19.01	7.60

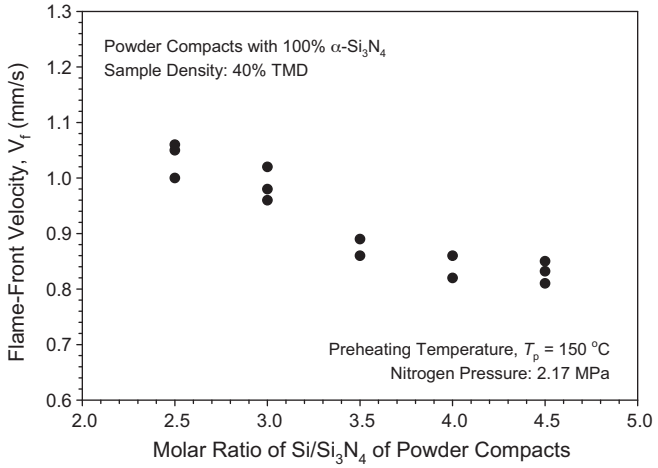

Fig. 2. Effect of molar ratio of Si/Si_3N_4 on flame-front propagation velocity of powder compacts with 100% α-Si_3N_4.

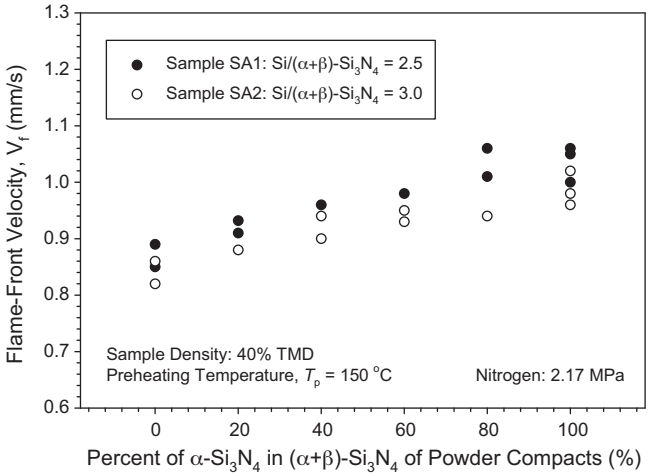

Fig. 3. Effect of molar proportion of α- to β-Si_3N_4 on flame-front propagation velocity of powder compacts with starting stoichiometries of SA1 and SA2.

triggered by a heated tungsten coil. Details of the experimental setup and measurement approach were reported elsewhere [30]. The microstructure of the synthesized product was examined under a scanning electron microscope (Hitachi S-3000N), and phase composition was analyzed by an X-ray diffractometer (Shimadzu XRD-6000) with Cu Kα radiation.

3. Results and discussion

3.1. Observation of combustion characteristics

Fig. 1(a) and (b) illustrates two series of combustion images recorded from the powder compacts with the same stoichiometry of SA1, but different α/β-Si_3N_4 proportions of 80/20 and 20/80. As shown in Fig. 1(a) and (b), the SHS process is characterized by one localized reaction zone spreading spirally along the sample. Instead of developing a planar combustion front propagating longitudinally, the presence of a spinning combustion wave implies that the synthesis reaction is not sufficiently exothermic [25]. According to Ivleva and Merzhanov [31], once the heat flux liberated from self-sustaining combustion is no longer adequate to maintain the steady propagation of a planar front, the combustion front forms one or several localized reaction zones. In the present study, the reduced reaction exothermicity stems most likely from the introduction of Si_3N_4 and AlN in the sample compact as the diluents, which are to suppress the melting of metallic reactants and to improve the degree of nitridation. Even though the sample SA1 contains the largest amounts of Si_3N_4 and AlN among all of the test specimens, a slight shrinkage of the burned product is evident in Fig. 1, signifying the melting of the metallic component on account of the high combustion temperature. Moreover, Fig. 1(a) indicates that for the sample with a higher proportion of α/β-Si_3N_4 (=80/20) the reaction zone travels at a faster rate in comparison to that shown in Fig. 1(b) with α/β-Si_3N_4 = 20/80. This is due to the formation of β-SiAlON with a less energy release compared to that of α-SiAlON when the β-Si_3N_4 is increased. As a result, the overall reaction exothermicity is reduced by increasing the β phase of Si_3N_4 in the reactant compact.

3.2. Measurement of flame-front propagation velocity and combustion temperature

The average combustion wave velocity (V_f) in the axial direction was determined from the recorded combustion sequence. For the powder compacts containing the α phase of Si_3N_4, Fig. 2 shows the variation of flame-front velocity with the Si/Si_3N_4 ratio of the sample. The flame velocity decreases from 1.06 to 0.81 mm/s as the Si/Si_3N_4 ratio increases from 2.5 (SA1) to 4.5 (SA5), which could be a consequence of the fewer uptake of nitrogen gas due to a lower degree of dilution causing further melting of the sample.

The influence of the phase of Si_3N_4 on combustion velocity is presented in Fig. 3 for the samples with starting stoichiometries of SA1 and SA2. An increase in the flame-front velocity with increasing proportion of α/β-Si_3N_4 was observed. In Fig. 3, the lowest combustion wave velocity of 0.82 mm/s was detected in the sample SA2 containing 100% β-Si_3N_4. This is attributed to the fact that in addition to α-SiAlON the introduction of β-Si_3N_4 leads to the formation of β-SiAlON, which reduces the overall reaction exothermicity. It is useful to note that on the synthesis of α- and β-SiAlON by combustion in gaseous nitrogen, the reaction enthalpy is mainly generated from nitridation of elemental Si and Al in the powder compact. Because it is impossible to have solid state combustion among Si, Al, Si_3N_4, AlN, and SiO_2, the SHS process should be sustained by the reactions involving gaseous nitrogen. Moreover, the content of nitrogen is lower for β-SiAlON than the α phase, which implies that the production of β-SiAlON through solid–gas combustion is less energetic. The estimated formation enthalpies of α- and β-SiAlON from the sample of this study are about 212 and 188 kJ/mol.

The composition dependence of combustion temperature is presented in Figs. 4 and 5, respectively showing the effects of the Si/Si_3N_4 and α/β-Si_3N_4 ratios. Due to the propagation of the com-

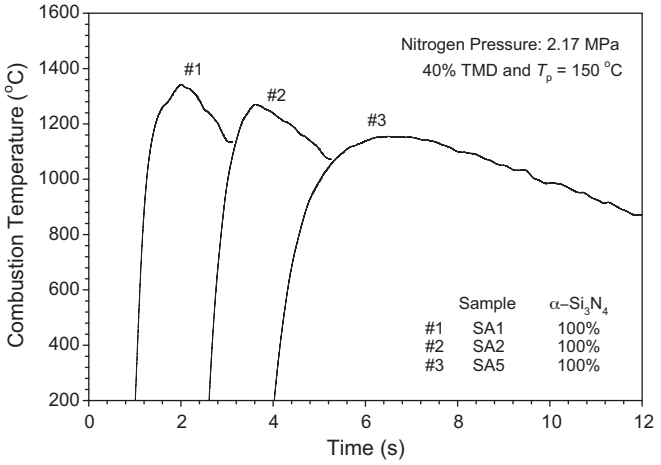

Fig. 4. Effect of molar ratio of Si/Si_3N_4 on combustion temperature of powder compacts with 100% α-Si_3N_4.

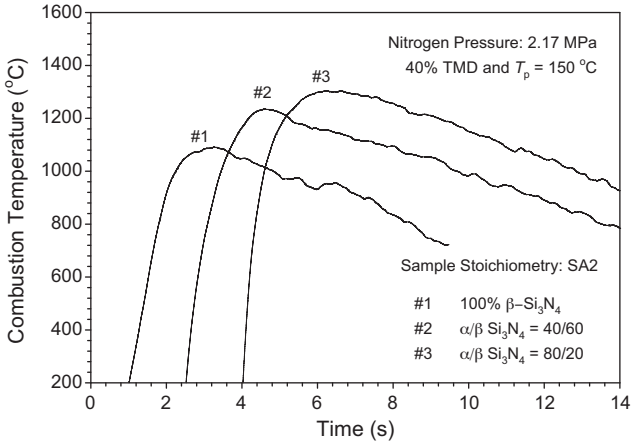

Fig. 5. Effect of contents of α- and β-Si_3N_4 on combustion temperature of powder compacts with a starting stoichiometry of SA2.

bustion wave, the temperature profile exhibits a rapid increase followed by a slow decline. The peak value corresponds to the combustion front temperature. Fig. 4 reveals that for the samples with 100% α-Si_3N_4, the temperature of the reaction front decreases from 1342 to 1154 °C, when the Si/Si_3N_4 ratio is augmented from 2.5 (SA1) to 4.5 (SA5). This confirms the variation of flame-front velocity with the molar ratio of Si/Si_3N_4.

The use of β-Si_3N_4 to replace α-Si_3N_4 lowered the combustion temperature as well. For example, the combustion front temperature of 1270 °C (profile #2 in Fig. 4) measured from the sample SA2 with 100% α-Si_3N_4 is higher than that (1091 °C) from the sample adopting 100% β-Si_3N_4 (profile #1 in Fig. 5). When a mixture of α- and β-Si_3N_4 was employed, as depicted in Fig. 5, a higher combustion temperature was observed in the sample with a larger proportion of α/β-Si_3N_4, which is in a manner consistent with that of the flame-front velocity.

3.3. Composition and morphology analysis of combustion products

Typical XRD patterns of the products synthesized from 100% α-Si_3N_4-containing powder compacts with different molar ratios of Si/Si_3N_4 are plotted in Fig. 6(a)–(d), within which the formation of α-SiAlON (JCPD card number: 84-0598) along with the presence of residual Si is identified. It was found that the amount of Si left unreacted increased obviously with increasing ratio of Si/Si_3N_4 in the sample. This implies incomplete nitridation of Si caused by an insufficient nitrogen uptake. It should be noted that no β phase of SiAlON was detected in the products synthesized from the samples with 100% α-Si_3N_4.

For the green samples containing a mixture of α- and β-Si_3N_4, as indicated in Fig. 7(a)–(c), the resulting products are (α + β)-SiAlON composites and the content of β-SiAlON (JCPD card number: 77-0755) increases with decreasing proportion of α/β-Si_3N_4. It is interesting to point out that even the sample with 100% β-Si_3N_4 also yields a composite of (α + β)-SiAlON and the corresponding XRD pattern is depicted in Fig. 7(d). Based upon the initial sample composition, the oxygen and nitrogen contents of α- and β-SiAlON formed in this study are about 3.6 and 53.6 mol% and 14.2 and 42.8 mol%, respectively. According to the intensity of specific XRD peaks associated with α- and β-SiAlON [13,32], the relative contents of these two SiAlONs formed in the final product were estimated. For the samples of SA1 and SA2 with 100% β-Si_3N_4, Fig. 8 reveals comparable amounts of α- and β-SiAlON (about 46–54%) formed in the final composites. When a mixture of (α + β)-Si_3N_4 was adopted, the increase of α-Si_3N_4 enhanced the formation of

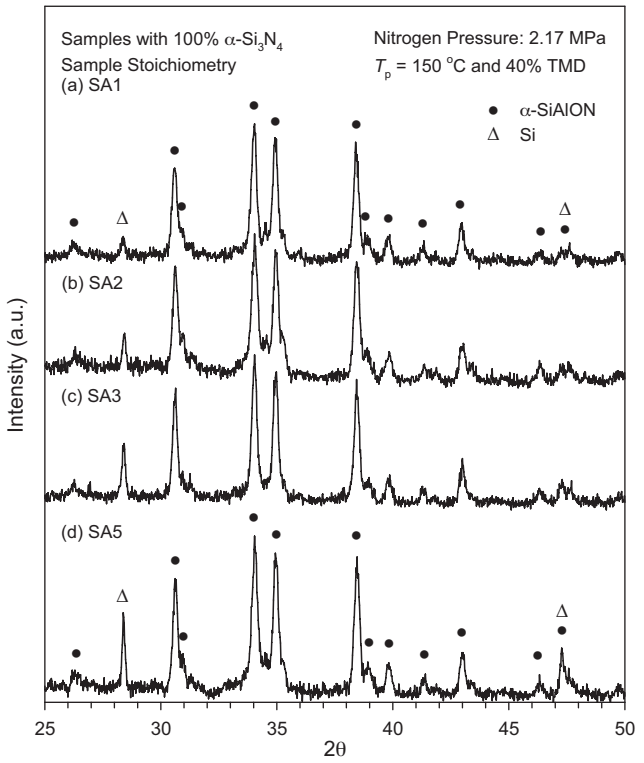

Fig. 6. XRD patterns of products synthesized from 100% α-Si_3N_4-containing powder compacts with different starting stoichiometries: (a) SA1, (b) SA2, (c) SA3, and (d) SA5.

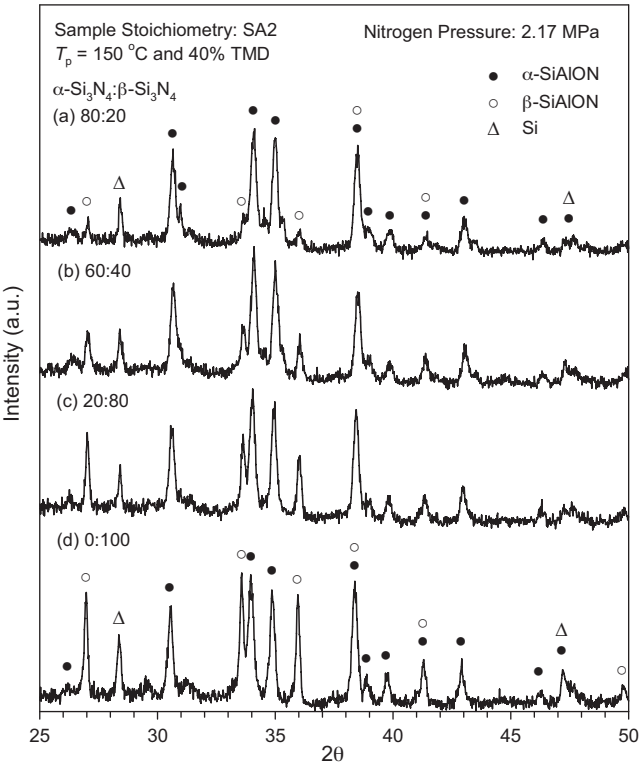

Fig. 7. XRD patterns of products synthesized from samples of SA2 with different proportions of α-Si_3N_4:β-Si_3N_4 = 80:20 (a), 60:40 (b), 20:80 (c), and 0:100 (d).

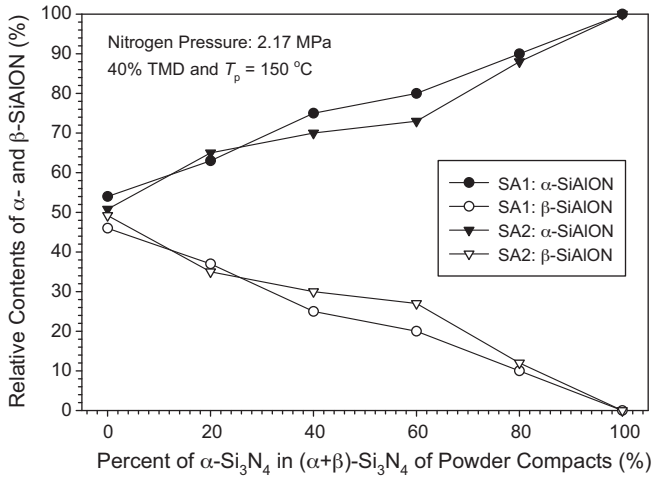

Fig. 8. Effect of proportions of α- to β-Si_3N_4 of powder compacts on relative contents of α- and β-SiAlON formed in final products.

α-SiAlON. As shown in Fig. 8, the content of α-SiAlON rises almost linearly to about 90% for the sample with α/β-Si_3N_4 = 80/20 and only the α phase of SiAlON is present in the case of using 100% α-Si_3N_4.

The morphology of the product synthesized from the sample of SA1 with 100% α-Si_3N_4 is illustrated in Fig. 9(a), showing α-SiAlON not only in the form of equiaxed crystals of 3–4 μm but also appearing as elongated grains of 8–10 μm and fine whiskers with a diameter of about 250–300 nm. This verifies the previous observation that combustion synthesis favored the growth of elongated α-SiAlON. As proposed by Liu et al. [18–20], the evolution of elongated and whisker-like α-SiAlON grains was governed by the vapor–liquid–solid (VLS) mechanism. For the sample adopting a mixture of α- and β-Si_3N_4, however, the resulting (α + β)-SiAlON composite exhibited a microstructure dominated by elongated grains with a high aspect ratio. Fig. 9(b) shows a typical SEM micrograph of the (α + β)-SiAlON composite obtained from the sample of SA1 with α/β-Si_3N_4 = 20/80. This suggests that simultaneous formation of α- and β-SiAlON promotes the growth of rod-like grains, probably because the elongated morphology is typical of β-SiAlON. In addition, the hardness (H_{v10}) of the as-prepared product is about 15.6 GPa. The fracture toughness (K_{1C}) is between 4.2 and 6.2 MPa $m^{1/2}$, which increases with increasing content of β-SiAlON in the final product.

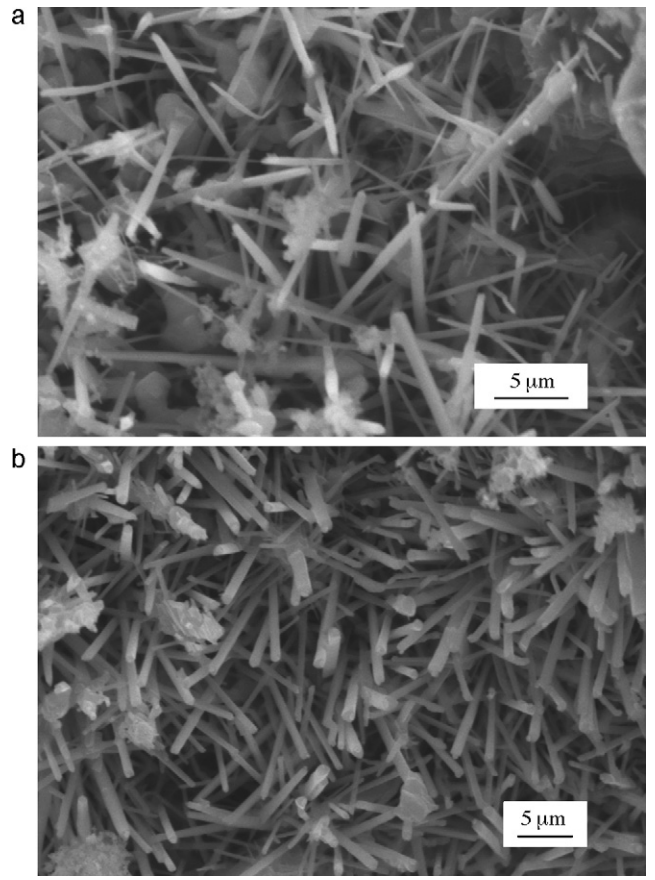

Fig. 9. SEM micrographs illustrating fracture surfaces of synthesized SiAlON from samples of SA1 with (a) 100% α-Si_3N_4 and (b) α/β-Si_3N_4 = 20/80.

4. Conclusions

The preparation of (α + β)-SiAlON composites was conducted by combustion synthesis in gaseous nitrogen of 2.17 MPa. The reactant compact was composed of Yb_2O_3, Si, Si_3N_4, SiO_2, Al, and AlN powders. The starting stoichiometry of the sample featured different molar ratios of Si/Si_3N_4 varying from 2.5 to 4.5. In particular, this study investigated the influence of the form of Si_3N_4, including α-Si_3N_4, β-Si_3N_4, and a mixture of (α + β)-Si_3N_4 with the proportion of α to β-Si_3N_4 ranging between 20/80 and 80/20.

Under a preheating temperature of 150 °C, self-sustaining combustion of the powder compact in nitrogen was achieved and the reaction zone propagated spirally along the sample. Due to the decrease of the reaction exothermicity caused by incomplete nitridation of Si, the combustion front was decelerated by increasing the molar ratio of Si/Si_3N_4 in the powder mixture. When compared to the sample with 100% α-Si_3N_4, the powder compact adopting 100% β-Si_3N_4 or a mixture of (α + β)-Si_3N_4 was subjected to a lower reaction temperature and thus a slower combustion wave.

For the powder compacts with 100% α-Si_3N_4, only the α phase of SiAlON was produced and as-synthesized α-SiAlON exhibited various morphologies including equiaxed crystals, elongated grains, and fine whiskers. When β-Si_3N_4 was adopted in the reactant mixture, however, both α- and β-SiAlON were formed in the final product. Moreover, the content of β-SiAlON in the synthesized (α + β)-SiAlON composite increased with increasing amount of β-Si_3N_4. In the case of using 100% β-Si_3N_4, a composite with comparable amounts of α- and β-SiAlON was obtained. Unlike the existence of various microstructures for α-SiAlON, the (α + β)-SiAlON composite exhibited a morphology dominated by elongated grains with a high aspect ratio.

Acknowledgement

This research was sponsored by the National Science Council of Taiwan, ROC, under the grant of NSC 98-2221-E-035-065-MY2.

References

[1] G.Z. Cao, R. Metselaar, Chem. Mater. 3 (1991) 242–252.
[2] T. Ekström, M. Nygren, J. Am. Ceram. Soc. 75 (2) (1992) 259–276.
[3] I.W. Chen, A. Rosenflanz, Nature 389 (1997) 701–704.
[4] H. Mandal, J. Eur. Ceram. Soc. 19 (1999) 2349–2357.
[5] V.A. Izhevskiy, L.A. Genova, J.C. Bressiani, F. Aldinger, J. Eur. Ceram. Soc. 20 (2000) 2275–2295.
[6] J.W.H. van Krevel, J.W.T. van Rutten, H. Mandal, H.T. Hintzen, R. Metselaar, J. Solid Sate Chem. 165 (2002) 19–24.
[7] X.W. Zhu, Y. Masubuchi, T. Motohashi, S. Kikkawa, J. Alloys Compd. 489 (2010) 157–161.
[8] X.W. Zhu, Y. Masubuchi, T. Motohashi, S. Kikkawa, T. Takeda, J. Alloys Compd. 496 (2010) 407–412.
[9] K. Shioi, N. Hirosaki, R.J. Xie, T. Takeda, Y.Q. Li, J. Alloys Compd. 504 (2010) 579–584.

[10] S.L. Hwang, I.W. Chen, J. Am. Ceram. Soc. 77 (1) (1994) 165–171.
[11] Z. Shen, T. Ekström, M. Nygren, J. Phys. D: Appl. Phys. 29 (1996) 893–904.
[12] G. Liu, K. Chen, H. Zhou, X. Ning, C. Pereira, J.M.F. Ferreira, J. Alloys Compd. 430 (2007) 269–273.
[13] M. Haviar, J. Eur. Ceram. Soc. 16 (1996) 665–670.
[14] C.R. Zhou, Z.B. Yu, V.D. Krstic, J. Eur. Ceram. Soc. 27 (2007) 437–443.
[15] M. Mitomo, M. Takeuchi, M. Ohmasa, Ceram. Int. 14 (1988) 43–48.
[16] T. Ekström, Z.J. Shen, K.J.D. MacKenzie, I.W.M. Brown, G.V. White, J. Mater. Chem. 8 (4) (1998) 977–983.
[17] M. Zenotchkine, R. Shuba, I.W. Chen, J. Am. Ceram. Soc. 87 (6) (2004) 1040–1046.
[18] G. Liu, K. Chen, H. Zhou, X. Ning, C. Pereira, J.M.F. Ferreira, Ceram. Int. 32 (2006) 411–416.
[19] G. Liu, C. Pereira, K. Chen, H. Zhou, X. Ning, J.M.F. Ferreira, J. Alloys Compd. 454 (2008) 476–482.
[20] G. Liu, K. Chen, H. Zhou, X. Ning, C. Pereira, J.M.F. Ferreira, J. Mater. Res. 20 (4) (2005) 889–894.
[21] G. Liu, K. Chen, H. Zhou, X. Ning, J.M.F. Ferreira, J. Eur. Ceram. Soc. 25 (2005) 3361–3366.
[22] X. Yi, T. Akiyama, J. Alloys Compd. 495 (2010) 144–148.
[23] X. Yi, K. Watanabe, T. Akiyama, Intermetallics 18 (2010) 536–541.
[24] K. Aoyagi, T. Hiraki, R. Sivakumar, T. Watanabe, T. Akiyama, J. Alloys Compd. 441 (2007) 236–240.
[25] C.L. Yeh, K.C. Sheng, J. Alloys Compd. 509 (2011) 529–534.
[26] A.G. Merzhanov, J. Mater. Process. Technol. 56 (1996) 222–241.
[27] Z.A. Munir, U. Anselmi-Tamburini, Mater. Sci. Rep. 3 (1989) 277–365.
[28] C.L. Yeh, in: H.J. Buschow, R.W. Cahn, M.C. Flemings, E.J. Kramer, S. Mahajan, P. Veyssiere (Eds.), Encyclopaedia of Materials: Science and Technology, Elsevier, Amsterdam, 2010.
[29] C.L. Yeh, in: M. Lackner (Ed.), Combustion Synthesis—Novel Routes to Novel Materials, Bentham Science, 2010.
[30] C.L. Yeh, Y.L. Chen, J. Alloys Compd. 478 (2009) 163–167.
[31] T.P. Ivleva, A.G. Merzhanov, Dokl. Physics 45 (2000) 136–141.
[32] P.O. Käll, Quantitative phase analysis of Si_3N_4-based materials, Chem. Scr. 28 (1988) 439–443.